Landmarks in Earth Reinforcement, Ochiai et al (eds),
©2001 Swets & Zeitlinger, ISBN 90 265 1852 8

Progressive pullout failure of geosynthetic reinforcement

J. Mak
Road and Traffic Authority, New South Wales, Australia
S-C.R. Lo
University College, University of New South Wales

ABSTRACT: Progressive pullout failure of geosynthetic reinforcement in pullout testing was studied by modelling the interface strain softening with a family stress transfer curves and finite difference formulation. The numerical adequacy of such analyses was checked. A parametric study was conducted to study the influence of various factors on the simulated mobilisation curves in pullout testing.

1 INTRODUCTION

Due to the elongation of a geosynthetic reinforcement under applied load, its displacement relative to the surrounding soil varies along the bonded length. When the relative displacement at the front zone is at a strain hardening state, the relative displacement at the rear zone is so minute that essentially nil interface shear stress is mobilised. When the interface shear stress at the rear zone reaches a significant value, the front zone is in a post-peak (hence strain softening) state. This leads to progressive pullout failure. Large scale pullout testing is considered to be a suitable method for studying the pullout behaviour of geosynthetic reinforcement, and a number of researchers have designed and commissioned large scale pullout testing equipment (Palmeira and Milligan, 1989; Juran et al., 1988; Fannin and Raju, 1993; and Farrag, et al., 1993, among others). Internal measurements, in the form of strain gauges or tell-tales mounted on the reinforcement, have been used by researchers to gain better interpretation of pullout test results and to examine the influence of box design on the measured progressive failure (e.g., Fannin and Raju 1993). Experimental studies are difficult because of the large number of factors that may influence the results and that large scale pullout testing is extremely resource intensive. Analytical studies have been performed to supplement such researches. These studies (e.g., Bergado & Chai 1994) were largely based on t-z curve analysis with strain softening soil springs of constant properties along the embedded length; and do not consider the evolution of stress non-uniformity of the surrounding soil induced by the pullout force (Raju et. al 1998). In theory, finite element analysis can capture the complete stress distribution in a pullout box. But modelling of strain softening plus the need to have the analysis proceeded to pullout failure, is problematic. A finite difference formulation was adopted in the analytical study reported in this paper. Such an approach enable easier modelling of interface strain softening. The broad objective of this study is to examine the progressive pullout failure of geosynthtic reinforcement in pullout testing under a wide range of conditions.

2 ANALYSIS MODEL

The layout of the modeled pullout box is shown in Fig. 1. The length of the pullout box was either 2m or 1m. However, the height of the box was 0.6 m irrespective of box length.

A flexible sleeve with a length equal to 10% of the box length was incorporated in the model. A flexible sleeve is defined as one with nil shear stress transfer between the reinforcement and the surrounding soil, but allows the reinforcement to deflect freely (and compatibly) with the soil in the vertical direction. The design of a flexible sleeve is reported in Lo (1998). It is different from a rigid sleeve which constrained the vertical displacement of the reinforcement to zero by a rigid device. As

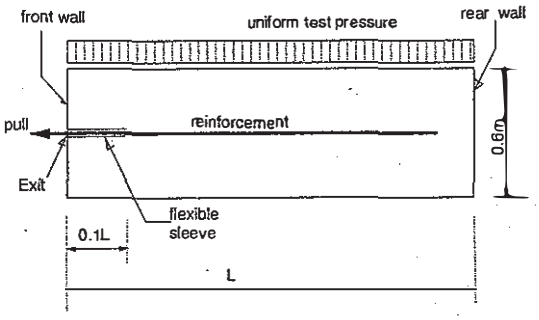

Figure 1. Pullout box layout

discussed in Raju et al (1998), a flexible sleeve arrangement gives a more uniform stress field. The front wall of the pullout box (i.e., the wall near exit sleeve) was taken either as a frictionless boundary or as a frictional boundary with an interface friction angle equal to 75% of the peak friction angle of the soil. The rear wall was considered as a roller boundary. To avoid the complication of investigating the boundary condition of the rear wall, the rear end of the reinforcement is at (0.1L+0.1m) from the rear wall. The bottom boundary was fixed whereas the top boundary was subject to a prescribed uniform test pressure. In this paper, only results corresponding to a test pressure of 50 kPa is presented.

The soil was modelled as a Mohr-Coulomb elastic-plastic material with a non-associated flow rule. Unless stated to the contrary, the soil parameters used in the analyses were: unit weight, γ = 20 kN/m^3; Young's modulus, E = 20 Mpa; Poisson's ratio, ν = 0.3; friction angle, ϕ = 40°; and dilation angle, ψ = 10°. The reinforcement was modelled as a linear elastic one-dimensional element. Four sets of reinforcement axial stiffness, J, of 300 kN/m, 500 kN/m, 800 kN/m and 1200 kN/m, were considered in this study. Shear springs at the reinforcement nodal points were used to model the interaction between the reinforcement and the surrounding soil. These shear springs had stiffness-strength characteristics described by a family of piecewise linear shear stress transfer functions as shown in Fig. 2a. The maximum shear stress was defined by the peak interface friction angle, δ_{peak}, which was assigned to be 30°. The fully strain softened shear stress was defined by the residual interface friction angle, δ_{resid}, which was assigned to be 21°. It is important to emphasise that δ_{peak} and δ_{resid} were element material properties, not scale dependent average properties as assumed in some simplified equation(s) for pullout calculating pullout resistance. The algorithm will select the appropriate piecewise linear function depending on the local interface normal stress, σ_n. Normal coupling springs of adequately high stiffness were also included in the numerical model.

The analyses were conducted using a finite difference stress analysis program known as FLAC, Fast Lagrangian Analysis of Continua (FLAC 1996). In FLAC, the equations of equilibrium and stress strain behaviour are expressed in finite difference form and are solved by an explicit iterative scheme. The analysis is inherently incremental and can model material strain softening without particular numerical difficulties. The program includes looping control commands and an internal programming language for implementing user-defined procedures. These features were used in the present study to incorporate interface strain softening, and to implement a displacement controlled mode of pullout. The latter ensured that the analysis can proceed beyond peak pullout failure. The smallest element size of 16mm wide by 20mm height, and each analysis had at least 600 displacement increments. For the sake of clarity, not all data points for every increment were plotted with a symbol.

The analysis required the prescription of horizontal stress, σ_h, at the initial state (ie, prior to the application of any pullout force). For a normally consolidated deposit, σ_h is commonly assessed by the equation $\sigma_h = (1-\sin\phi)\sigma_v$, where σ_v is the vertical stress. In a retaining wall, the effect of compaction at shallow depth leads to a horizontal stress considerably higher than that given by the above equation, and may even approach the passive pressure value (Ingold, 1979). Lo (1998) conducted pullout tests with a pre-loading pressure applied prior to the application of test pressure so that the effects of vertical compaction stress could be at least partly simulated. In this study, the initial earth pressure coefficient was taken as 1.0, unless stated otherwise to the contrary.

The stability of the analysis was verified by simulating a pullout test with J=500x10^3 kN/m. With

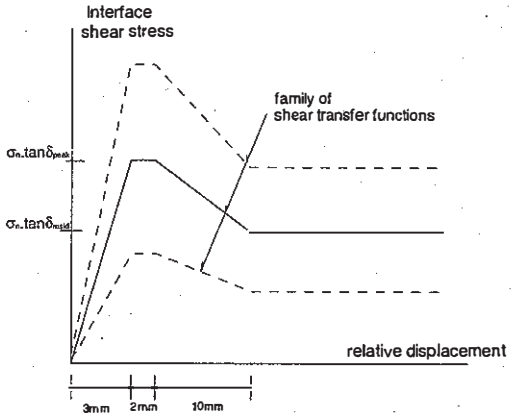

(a) Shear stress transfer function

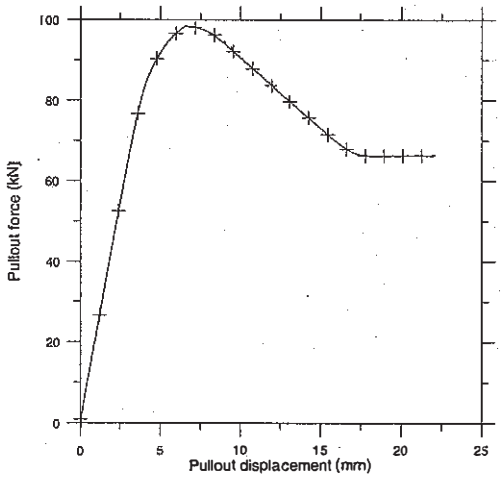

(b) Simulated response for quasi-inextensible reinforcement

Figure 2. Interface shear stress transfer

such a high reinforcement stiffness, reinforcement elongation is negligible and the peak pullout force should be the integration of peak interface shear stresses over the bonded length of the reinforcement. The pullout force displacement curve should also be similar to that of the shear spring characteristics (Fig. 2a). The simulated force displacement curve presented in Fig. 2b evidently conformed with these "known" results.

It is important to emphasise that the material models and parameters adopted in this study were not specific to any particular soil or reinforcement. It is not the intention of this paper to quantitatively predict the response in a pullout testing. These were reasonable assumptions so that the complicated behaviour pattern, in particular the influence of test conditions, can be better understood.

3 RESULTS OF REFERENCE CASE

The reference case is defined as a pullout box of engthe 2m with a smooth front wall, under 50 kPa test pressure and J = 500 kN/m stiffness. These conditions were considered as reasonable and probably induce slightly higher progressive failure relative to high strength/stiffness reinforcement used in reinforced soil structures. Hence the analysis results of the reference case were examined in detail.

3.1 *Force displacement behaviour*

The reinforcement pullout force displacement curve was presented in Fig. 3 (plot with filled-box symbol) using mobilization factor (MF) defined as:

$$MF = P / (2 \sigma_{vo} L_b \tan \delta_{peak}) \quad (1)$$

where P = pullout force (at exit location), σ_{vo} = pressure applied at the top boundary plus vertical stress due to the self weight of 0.3m height of soil, L_b = initial bonded length of reinforcement.

In general $1 \geq MF \geq \tan(\delta_{resid})/\tan(\delta_{peak})$. The upper bound value of unity applies when the reinforcement can be considered as inextensible, whereas the lower bound value was for the residual pullout resistance. To eliminate any aberration of the mobilisation curve due to elongation of the unbonded reinforcement (within the sleeve), the reinforcement displacement at the beginning of the bond length (i.e., at 0.1L from the exit) is plotted in this figure. A maximum pullout force of 71 kN (MF=0.717) was mobilized at 130 mm pullout displacement. The peak pullout force was lower than that given by the peak interface strength, as expected, but higher than that given by the fully softened interface strength. Once the peak pullout force was achieved, further application of displacement at the reinforcement front end led to a rapid reduction

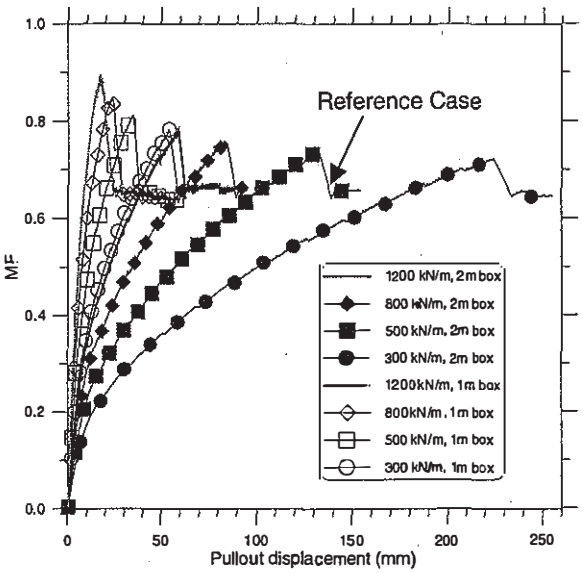

Figure 3. Pullout force displacement responses

of pullout force to 64 kN (MF=0.646), which corresponded to that given by a fully softened interface strength.

The force displacement curve so predicted conformed to known trend obtained from large scale pullout testing, with the exception of the rapid reduction of the peak pullout force to a residual value. However, most pullout tests were terminated at less than 130mm displacement, and therefore may not have captured the rapid reduction of peak force to a residual value. This rapid drop in pullout force from peak value to fully softened value appears to be related to the decrease in the reinforcement tension and elongation after peak pullout force. When the reinforcement was pulled beyond the maximum pullout force, the reduction in reinforcement tension led to a reduction in the elongation of the reinforcement. Since the displacement at the reinforcement front end was prescribed as increasing, other points along the reinforcement had to move forward further and thus inducing further strain softening of the interface shear stress.

3.2 *Stress distribution*

The distribution of vertical stress changed with application of pullout force as illustrated in Fig. 4a. At P = 35 kN (ie, ~ 50% of maximum pullout force), the normal stresses acting on the reinforcement (σ_n) were smaller than the average overburden stress (56 kPa) within the front region defined hy a distance of less than 0.5 m of the pullout box. In the mid region, defined by a distance of about 0.5 m to 1.4 m from the front wall, σ_n was higher than the average overburden stress and had a maximum value of 61 kPa. In the rear region, defined by a distance greater than 1.4 m behind the front wall, σ_n was essentially equal to the average overburden stress.

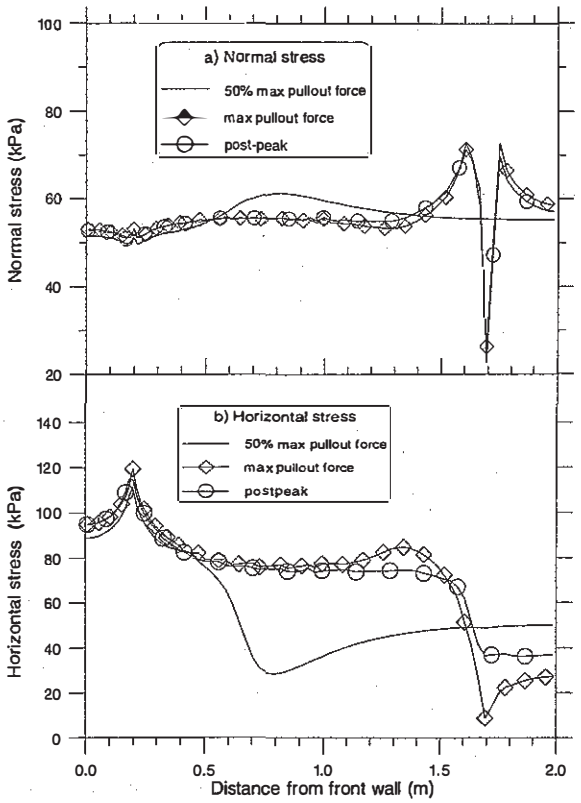

Figure 4. Stress distribution at mid-height of pullout box

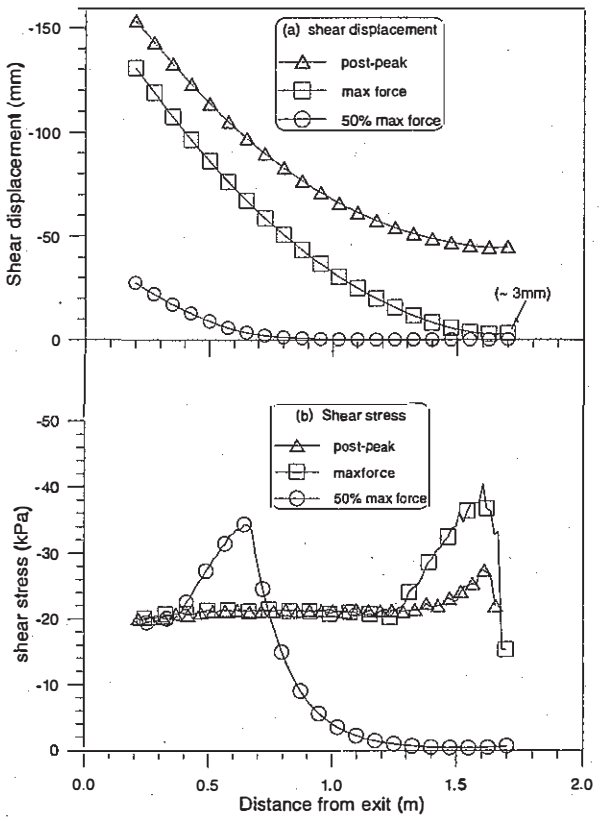

Figure 5. Shear displacement and interface shear stress of reinforcement

At maximum pullout force, σ_n within the front region of the pullout box remained essentially the same as above. In the mid region, σ_n was close to the average value. σ_n in the rear zone was highly non-uniform. σ_n increased rapidly between the distance of 1.4 m to 1.6 m. It reduced sharply to 30 kPa at the rear end of the reinforcement, but σ_n jumped back to 72 kPa slightly behind the rear end of the reinforcement. When the pullout force was at the residual value, the σ_n distribution along the reinforcement was similar to that at peak pullout force.

The rapid reduction of σ_n in the rear zone of the reinforcement can be explained by looking at the distribution of horizontal stress as presented in Fig. 4b. The pullout force led to reduction in horizontal stress in the rear zone of the reinforcement. At maximum pullout force, the horizontal stress was reduced to such a low value that the soil elements approached failure, which in turn limited the value of vertical stress.

3.3 *Relative displacement and interface shear stress*

The shear displacement of the reinforcement (ie relative to the surrounding soil) was presented in Fig. 5a, whereas the interface shear stress was presented in Fig. 5b. At P = 35 kN, ie ~50% of maximum pullout force, shear stress and displacement along a significant part of the reinforcement were essentially zero. Peak shear stress occurring at about 0.6m from the exit. This implies significant strain softening had already occurred along the front portion. Therefore, the relevance of modelling interface strain softening was demonstrated.

Maximum pullout force occurred with slippage of the rear end of the reinforcement, as indicated by a shear displacement of about 3mm. A significant portion of the embedded length, however, had attained the fully softened state. The maximum interface shear stress at maximum pullout force was slightly higher than that at P=35 kN. At residual pullout force, the interface shear stress along nearly the entire bonded length was at the fully soften state but there was a "small peak" near the rear end of the reinforcement. Both phenomena was due to stress non-uniformity induced by the pullout force.

4 INFLUENCE OF REINFORCEMENT STIFFNESS AND BOX LENGTH

The influence of reinforcement stiffness was examined by conducting the analysis for different J values of 1200kN/m, 800 kN/m and 300 kN/m. The mobilisation curves so obtained were compared to that of the reference case (J= 500 kN/m). As evident from

Fig. 3, the reinforcement stiffness has a slight influence on the peak mobilised value but a significant influence on the rate of mobilisation.

The effect of box length was studied by repeating the analyses for a 1m box. As evident from Fig. 3, the shorter box gave a higher peak mobilised value and a significantly higher rate of mobilisation. This is in agreement with known trend deduced experimentally (Fannin and Raju 1993). The mobilisation curves of the shorter box also appeared to be less sensitive to the reinforcement stiffness, J.

5 INFLUENCE OF SOIL STIFFNESS

The analysis for 2m box was repeated for a range of soil stiffness with E varying from a low value of 8.33 MPa to a high value of 100 MPa, but with J kept at 500 kN/m. This means the J/E ratio was varied. It is sometimes assumed that the effects of change in either J or E can be approximated by changes in J/E ratio. As evident from the mobilisation curves presented in Fig. 6, change of J/E caused solely by change in E had minimal influence on the mobilisation of pullout resistance. This was very different from change in J/E caused by change in J but with E kept constant (see Fig. 3).

6 INFLUENCE OF FRONT WALL AND SLEEVE DESIGN

The influence of the front wall roughness and the provision of sleeve were also examined by conducting the following additional analyses for the 2m box.

- flexible sleeve and a rough front wall,
- rigid sleeve and a smooth front wall,
- rigid sleeve and a rough front wall,

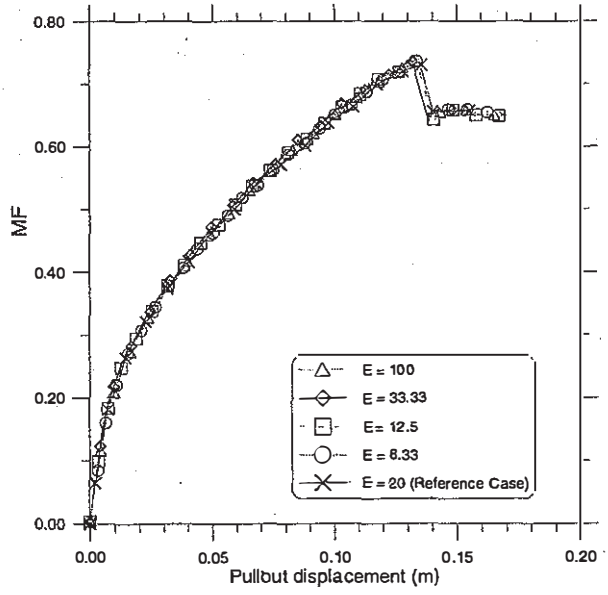

Figure 6. Influence of soil stiffness

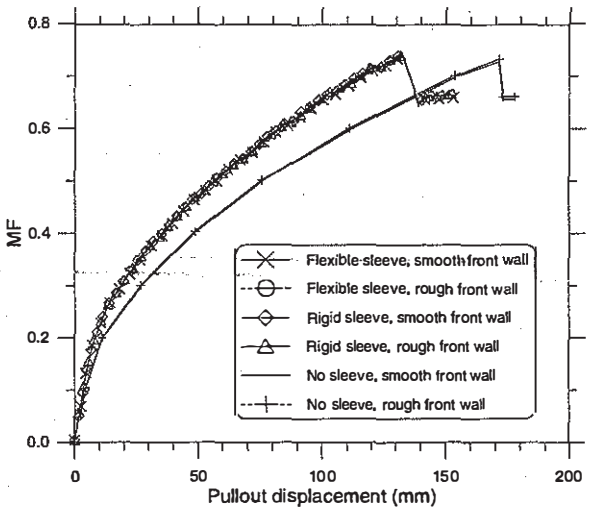

Figure 7. Influence of sleeve and front wall

- no-sleeve and a smooth rough front wall,
- no-sleeve and a rough front wall.

The mobilisation curves for these six cases were presented in Fig. 7. The curves obtained from the first three conditions were essentially the same as the reference case of flexible sleeve and smooth front wall. The curves for the two cases for no-sleeve, however, manifested slightly higher pullout displacement. This is due to the additional 0.2m in reinforcement length due to the elimination of sleeve. This finding conformed to that obtained by Raju et al (1998) based on a synthesis of a limited experimental results.

7 INFLUENCE OF NUMERICAL MODELLING

The assumption of an initial horizontal to vertical stress ratio, K_i, of unity is somewhat arbitrary although tenable. Therefore, the reference case was re-analysed with $K_i = 0.75$ and $K_i = 0.5$. As evident from Fig. 8, The resultant mobilization curves are essentially identical to that of reference case.

It is also recognised that friction angle may increase at lower confining stress. To model this effect the variation of friction angle with confining stress in triaxial testing was predicted by Lade's failure criterion (Lade 1977) reproduced as Eqn (2).

$$\left(I_1^3/I_3 - 27\right)\cdot\left(I_1/p_a\right)^m = \eta \qquad (2)$$

where I_1 and I_3 are the first and third stress invariance, p_a is the standard atmospheric pressure, and η and m are soil parameters. $\eta = 65$ and $m = 0.35$ was adopted which then gave $\phi = 40^o$ at p_a. An increase in friction angle will lead to a corresponding increase in dilatancy angle, ψ and this was modelled using the relationship proposed by Bolton (1985)

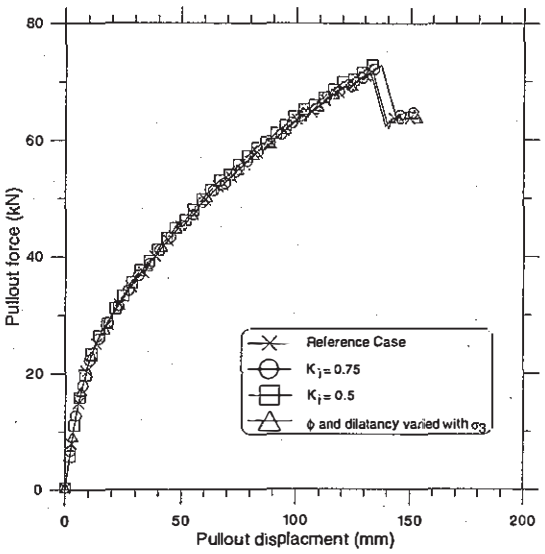

Figure 8. Influence of numerical modelling

$$\phi = \phi_{cv} + 0.8\psi \quad (3)$$

where ϕ_{cv} is the friction angle at critical state and a value of 32° was adopted in the analysis. Despite all these changes, the mobilisation curves for these three analyses were essentially identical to that of the reference case as evident from Fig. 8.

8 SUMMARY AND CONCLUSIONS

Progressive pullout failure in pullout testing of geosynthetic reinforcement was studied analytically by modelling interface strain softening with finite difference analysis. Despite a uniform stress was prescribed at the upper boundary, the normal stress on the reinforcement became non-uniform due to the application of the pullout force. Therefore, interpretation of internal force and displacement measurements would be difficult unless internal distribution of normal stresses is also measured.

A parametric study was conducted to study the effects of different factors on simulated mobilisation curve. Increasing J and/or decreasing pullout box length led to higher peak MF value, considerably higher rate of mobilisation, and an apparently slower rate of strain softening of the pullout force after the peak. Changes in soil stiffness, E, however, had a minimal effect on the simulated mobilisation curves. The front wall roughness and sleeve design were also found to have only slight influence on the simulated mobilisation curves.

Two modelling factors, (i) the value of K_i, and (ii) changes in ϕ and ψ with σ_3, were also studied. Both soil modelling factors had minimal influence on the simulated mobilisation curves.

9 ACKNOWLEDGEMENT

The authors wish to thank the Roads and Traffic Authority, New South Wales, Australia, for allowing the first author in participating in the publication of this paper. The opinions and findings expressed in the paper are, however, solely those of the authors.

REFERENCES

Bergado, D.T. and Chai, J. (1994) "PulloutForce/Displacement Relationship of Extensible Grid Reinforcement". *Geotextiles and Geomembranes*, 13, 1994, 294-316.

Bolton M.D. (1986). The strength and dilatancy of sand. Geotechnique, 36[1], 65-78.

Fannin, R. J., and Raju, D. M. (1993). On the pullout resistance of geosynthetics. *Canadian Geotechnical Journal*, Vol. 30, June 1993, pp. 409 - 417.

Farrag, K., Acar, Y.B. and Juran, I. (1993). "Pullout resistance of geogrid reinforcement". *Geotextiles and Geomembranes*, **11** (2): 133-159.

FLAC (1996) "Fast Lagrangian Analysis of Continua", Version 3.3. Theory and background. Itasca Consulting Group.

Ingold (1979). The effects of compaction on retaining walls. Geotechnique, **29**: 265-283.

Juran I., Knochenmus G., Acar Y.B., and Arman A. (1988). Pullout response of geotextiles and geomembranes. Proc Symposium on Geposynthetics for Soil Improvement, ASCE, Tennessee, 92-111.

Lade P.V. (1977) Elastoplastic stress strain theory for cohesionless soils with curved yield surfaces. *J of Structures*, Vol. 13, 1019-1035.

Lo, S-C.R. (1998). "Pull-out resistance of polyester straps at low overburden stress". *Geosynthetics International*, **5** (4): 361-382.

Palmeira, E.M. and Milligan, G.W.E. (1989). "Scale and other factors affecting the results of pull-out tests of grids buried in sand". *Geotechnique*, 39 (3): 511-524.

Raju D.M., S-C.R. Lo and Gopalan M. (1998) "On large scale pullout testing". *Geotechnical Eng J of SE Asian Geot. Society*, **29** (4).

Landmarks in Earth Reinforcement, Ochiai et al. (eds),
© 2001 Swets & Zeitlinger, ISBN 90 2651 863 3

Strain-induced toughness and shearing characteristics of short-fiber reinforced soils

Katshuhiko Makiuchi & Kunio Minegishi
Department of Transportation Engineering and Socio-Technology, College of Science & Technology, Nihon University, Japan

ABSTRACT: In order to study the quantitative effects of short-fiber reinforced soils on shear behaviors, a series of box shear test and unconfined compression test on non-cohesive and cohesive soils were carried out. Reinforcement materials used in the tests were consisted of synthetic fibers with different sizes and surface friction properties. It was found from the experimental works that length, diameter and surface roughness of fibers had marked effects on mechanical properties of the reinforced soils and the recommended optimum mixing rate of the short fibers was presented. Furthermore test results showed the prominent increase in peak shear resistance of fiber-reinforced soils and their high residual strength within the wide range of large deformation. Its strain-induced toughness can be recognized as effective and well-directed for earthquake-proof geotechnical structures.

1 INTRODUCTION

A short-fiber reinforced-earth construction method is recently developed in attempting to use for unstable embankment slopes and poor ground foundations, and in particular for the backfill soils of wall-type reinforced-earth with the aim of strengthening the shear resistance. However theoretical and experimental reinforcement mechanism and fundamental mechanical properties of fiber-soil mixture are not made fully clear at present. Interface friction among soil particles and fibers and their interlocking or intertwine action are considered as fundamental factors of improvement of fiber-reinforced soil which is called as an internal confining reinforcement in this paper.

The fiber-reinforced techniques has some advantageous engineering properties of soft grounds and filling materials. For example, the fiber-reinforced soil construction method can be applied for purposes of supplying an apparent cohesion component for non-cohesive granular sandy soils. Furthermore it can be used for controlling the engineering properties of problematic soils for stabilizing geotechnical structures and for vegetation, erosion control of earth slopes, weak disposal soil materials and so on.

There are two major types of earth-reinforcement techniques using synthetic fibers. One is a widely used conventional method in which continuous filament yarns are employed for non-cohesive granular soils, for example, *Texsol* product (Public Works Research Center, 1992) developed firstly in French. In this type the filaments are mixed with fine sand at the specified moisture content by the jet-mixing equipment and the fiber-sand mixture is built up in the field. Another type is a recently developing method using short length fibers (Research Institute of Public Works, 1997). As the results of improvement, the fiber-reinforced soils acquires extremely high ductility and toughness against the deformation of geotechnical structures and contributes to reduce the lateral earth pressure within embankments and back-fill soils.

Some interaction effects among soils types, shape, size and surface roughness of reinforcement materials are commented in other reports (Research Institute of Public Works, 1997 and Nakahara,H., 1998). In this experimental works mechanical properties of fiber-reinforced fine sand and sand-clay mixture were investigated using both a laboratory shear box test and an unconfined compression test.

2 MATERIAL CHARACTERIZATION

2.1 *Soils*

Two types of soils; *Toyoura* fine sand (abbreviation: S) and *Kaolin* clay (abbreviation: K) were used for this experimental works. Physical characteristics of the fine sand were; particles density $\rho_s = 2.64$ g/cm.^{3} 60 % passing gain diameter $d_{60} = 0.2$ mm, uniformity coefficient $Uc = 2.0$, coefficient of curvature $Uc' = 1.45$, maximum and minimum void ratios $e_{max} = 0.97$, $e_{min} = 0.59$, respectively. Physical properties of the clay (CH: high plasticity clay) were; particles density $\rho_s = 2.56$ g/cm^3, liquid limit $w_L = 85.1$ %, plasticity index $Ip = 54.6$.